Polymer Chemistry

ROYAL SOCIETY OF CHEMISTRY

PAPER

View Article Online
View Journal | View Issue



Cite this: *Polym. Chem.*, 2023, **14**, 5260

# Melt memory in propene–pentene isotactic copolymers: the case of defects hosted in the crystals†

Fabio De Stefano, *[a] Alessandra Cicolella, [a,b] Annachiara Barreca,[a] Miriam Scoti [a] and Claudio De Rosa *[a]

The memory of the crystalline state in the melt of propene–pentene isotactic copolymers (iPPC5) has been analyzed. Samples with pentene concentrations varying from 0.5 to 12.4 mol% have been prepared with a highly stereoselective metallocene catalyst. Pentene comonomeric units are largely included in the crystals of the polymorphic forms of isotactic polypropylene (iPP) and the relative amount of included comonomer increases with increasing pentene concentration, inducing crystallization of the trigonal δ form of iPP when the pentene content exceeds about 9–10 mol%. Self-nucleation experiments have demonstrated that high concentrations of pentene units produce a remarkable melt-memory that persists up to temperatures much higher than the melting temperature. The width of Domain II, where self-nucleation occurs, and the difference between the temperature of the beginning of the homogeneous melt, where the melt-memory is erased, and the melting temperature increase with increasing pentene concentration. These data indicate that a remarkable melt-memory of iPP crystals exists not only for the known cases of copolymers of iPP with noncrystallizable comonomers but also when comonomers are largely included in the crystals. Crystallization from a heterogeneous melt containing self-nuclei favors crystallization of the γ form, whereas crystallization from a homogeneous melt favors crystallization of the α form. For a high pentene concentration of 12.4 mol%, the trigonal δ form crystallizes from the homogeneous melt, whereas a small amount of the α form crystallizes from the heterogeneous melt when self-nucleation occurs and no trace of the γ form is observed.

Received 27th September 2023,
Accepted 8th November 2023

DOI: 10.1039/d3py01086d

rsc.li/polymers



## Introduction

The control of the crystallization process of semi-crystalline polymers represents a crucial step that affects the final properties of the material. Polymer crystallization proceeds through two main steps: nucleation followed by a subsequent growth process. Several strategies have been developed over the years to control and enhance the nucleation rate including epitaxy,[1–4] use of nucleating agents,[2] application of external stimuli,[5,6] and self-nucleation processes.[7–11] In particular, self-nucleation (SN) consists of a thermal protocol that allows increasing the nucleation density of a polymer by several orders of magnitude through the production of self-nuclei or self-seeds in the melt.[9–11]

Self-nucleation exploits the intriguing concept of the presence in the polymer melt of a memory of the preceding crystals that remain alive surviving melting even upon heating at temperatures higher than the end of the melting process. The melt-memory is revealed by the evidence that crystallization by cooling from this nonisotropic melt occurs at temperatures higher than that observed when crystallization occurs from an isotropic melt heated at very high temperatures, where any memory of the crystalline state has been deleted.[9–11] The increase in the crystallization temperature indicates that during crystallization self-nucleation occurs because self-nuclei or self-seeds survive in this nonisotropic melt.[11]

Based on this concept, a SN thermal protocol has been developed allowing the definition of the temperature ranges for which the melt of a polymer is a homogeneous melt (Domain I, at very high temperatures, generally higher than the thermodynamic melting temperature), a heterogeneous

[a]*Dipartimento di Scienze Chimiche, Università di Napoli Federico II, Complesso Monte S. Angelo, Via Cintia, I-80126 Napoli, Italy. E-mail: claudio.derosa@unina.it, fabio.destefano@unina.it*
[b]*Scuola Superiore Meridionale, Largo San Marcellino 10, I-80138 Napoli, Italy*

†Electronic supplementary information (ESI) available: Experimental details of synthesis and characterization by DSC and X-ray diffraction. WAXS profiles of the samples crystallized from the melt. Results of self-nucleation experiments on all samples of iPPC5 copolymers. See DOI: https://doi.org/10.1039/d3py01086d

melt (Domain II, at lower temperatures) containing self-nuclei (Domain IIa) or self-seeds (Domain IIb), or a melt containing crystal fragments (Domain III, at very low temperatures).[9–11]

The self-nucleation behaviors of a variety of classes of homopolymers, copolymers and polymer blends have been described and reviewed by Muller and Cavallo.[11] The origin of melt-memory and the nature of self-nuclei have been largely debated and several possible hypotheses have been suggested depending on the specific polymer, as residual orientation and/or conformational order of the chains,[10–17] or aggregates of portions of chains generated by some interactions in the melt.[11,14,18–20] In particular, the presence of a melt-memory that survives up to high temperatures and very large Domain IIa have been observed in various classes of polymers,[11] and in most cases of homopolymers they have been ascribed to the presence of intermolecular interactions,[11,14,18–20] as in poly(amide)s and polyesters showing dipole–dipole interactions or hydrogen bonds.[11,21,22] Accordingly, polyolefins generally show, instead, weak memory effects and sharp Domain IIa.[10,23]

The case of apolar polyolefin homopolymers and random polyolefin copolymers is particularly puzzling. In fact, as already stated, polyolefin homopolymers, such as polyethylene (PE) and isotactic polypropylene (iPP), show weak memory effects and sharp Domain IIa,[10,23] but, surprisingly, copolymers of PE and iPP have shown, instead, a remarkable melt-memory and broad Domain IIa.[11,15,23–28]

This different behavior of copolymers has been attributed to the presence of noncrystallizable comonomers mainly rejected from the crystals and to the consequent selection of crystallizable sequences during crystallization.[23,24] In particular, a significant melt-memory effect, which persists at temperatures higher than the thermodynamic melting temperature has been found in ethylene/1-butene copolymers,[23] in contrast with the PE homopolymer. Reid *et al.*[23] attributed this result to the formation of a special amorphous phase upon crystallization of statistical copolymers with noncrystallizable comonomers associated with the partitioning of crystallizable sequences of suitable lengths. Comonomers of big sizes are rejected from PE crystals and, therefore, crystallization of statistical copolymers occurs through early selection of long regular ethylene sequences, whereas other shorter regular sequences segregated in the melt diffuse towards the growing crystal to deposit and continue the growth of the lamellae. This produces a special structure of the melt with the formation of knots, loops and ties.[23] During melting, these topological constraints and branches hamper melt diffusion to randomize all sequences and clusters of initial crystalline sequences remain in the melt and are erased only at very high temperatures.[23,24] These clusters represent the self-nuclei present in Domain IIa that account for the melt-memory persisting up to high temperatures. Analogous behaviors have been obtained for other random ethylene copolymers with longer 1-alkene, such as 1-hexene.[24]

A remarkable melt-memory and broad Domain IIa have also been found in statistical copolymers of iPP with ethylene[15] and, more recently, in copolymers with a polar bulky comonomeric unit,[25] in contrast with the weak memory effect and very narrow Domain II observed in the iPP homopolymer.[9] These observations have been again interpreted with the mechanism of partitioning of sequences proposed by Reid *et al.*,[23] and the formation of a sort of constrained melt. In propene–ethylene copolymers, the formation of this constrained self-nucleated melt has also been demonstrated by the experimental observation that the self-nucleated melt in Domain II shows a rheological behavior different from that of the isotropic melt,[15] indicating different chain dynamics. Furthermore, in the copolymers bearing the bulky polar comonomeric units that are rejected from the crystals and produce more topological restrictions in the melt than ethylene, the possible interaction between polar groups contributes to further restrict the diffusion of the crystallizable sequences.[25]

Therefore, the different behaviors of polyolefin homo- and copolymers are generally attributed to the presence of non-crystallizable comonomers that produce restrictions in the melt,[15,23] but various points about the self-nucleation and the melt-memory effect in polyolefins are still unclear. In particular, the effect of crystallizable comonomers included in the crystals of the iPP homopolymer has never been discussed. In this paper, we have analyzed the self-nucleation in copolymers of iPP with pentene that, notwithstanding the large size, are included in the crystals of the polymorphic forms of iPP to a very large extent. This system provides an opportunity to demonstrate that the melt-memory in polyolefins is not necessarily associated with noncrystallizable comonomers and to verify the effect of the hypothesized partitioning of regular crystallizable sequences.

Isotactic propylene–pentene copolymers (iPPC5) show a unique polymorphic behavior that is mostly due to the inclusion of pentene comonomer units in the crystals.[29–38] In fact, the amount of pentene units included in the crystals of the α form depends on the total pentene content of the copolymer and strongly increases at high pentene concentrations. In copolymers with low pentene concentration (up to 5–6 mol%), pentene comonomer units are in part included in the crystals and act as defects inducing crystallization of the α and γ forms. This is demonstrated by the increase in the dimensions of the unit cell of the crystals of the α form.[29,31] The inclusion of pentene as defects in the crystals leads to, as expected, a decrease of crystallinity and melting temperature of the defective crystals of the α form with increasing pentene concentration.[29–38] For higher pentene concentrations, many more pentene units are included in the crystals of the α form, and at a threshold concentration of 8–9 mol%, a remarkable increase in density occurs which induces the crystallization of the trigonal δ form.[29,31] In the crystals of the trigonal δ form, pentene units are no longer defects but they act as a structural feature contributing to the change in the crystallized polymorphic form, from the monoclinic α form to the trigonal δ form.[29,31] In this case, pentene units co-crystallize in a new polymorphic form, the trigonal δ form, that, in fact, never crystallizes in the iPP homopolymer.[29,31]

In this study, the effect of the presence of cocrystallizable pentene comonomer units on the self-nucleation behavior of iPP has been examined and the effect of the presence of a memory in the melt on the complex polymorphic behavior of iPP has been analyzed.

## Experimental part

Samples of the iPP homopolymer and iPPC5 copolymers were synthesized by using the metallocene pre-catalyst dimethylsilyl (2,2′-dimethyl-4,4′-diphenylindenyl)$ZrCl_2$ as reported in Chart 1 activated with methylalumoxane (MAO), according to the method described in the ESI.† All the analyzed samples are listed in Table 1. The samples are characterized by similar molecular masses and comonomer concentrations between 0.5 and 12.4 mol%. The catalyst is highly stereoselective, consistent with the $C_2$-symmetry of the zirconocene complex, and produces highly isotactic samples of the iPP homopolymer with negligible concentrations (lower than 0.1 mol%) of stereodefects, represented by *rr* triad stereosequences, and a small amount of nearly 0.2 mol% of regiodefects, represented by secondary 2,1-erythro propene units.[39] Similar high stereoregularity is observed in the copolymers at any comonomer concentration. This microstructure allows studying the only effect of pentene comonomeric units on the crystallization and self-nucleation behaviors of iPP.

The details of calorimetric measurements, self-nucleation experiments and of the characterization by X-ray diffraction are reported in the ESI.†

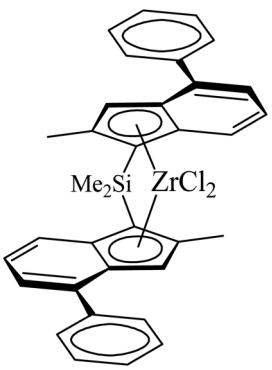


**Chart 1** Zirconocene pre-catalyst used in the propene–pentene copolymerization.

**Table 1** Pentene concentrations, molecular masses ($M_w$), polydispersities of the molecular mass (PDI), melting temperatures of as-prepared ($T_m^I$) and melt-crystallized ($T_m^{II}$) samples and crystallization temperatures ($T_c$) of samples of iPP (sample iPP25) and iPPC5 copolymers

| Sample | Pentene[a] (mol%) | $M_w$ (kDa) | PDI | $T_m^I$ [b] (°C) | $T_c$ [b] (°C) | $T_m^{II}$ [b] (°C) |
|---|---|---|---|---|---|---|
| iPP25 | 0 | 680 | 2.0 | 162.3 | 115.4 | 159.8 |
| iPPC5-1 | 0.55 | 1016 | 3.5 | 153.1 | 112.0 | 149.8 |
| iPPC5-2 | 2.0 | 504 | 2.1 | 136.9 | 99.2 | 134.4 |
| iPPC5-3 | 3.7 | 472 | 1.8 | 126.6 | 86.2 | 124.2 |
| iPPC5-4 | 6.8 | 326 | 2.1 | 104.2 | 59.1 | 102.4 |
| iPPC5-5 | 10.5 | 374 | 2.1 | 84.7 | 41.3 | 79.3 |
| iPPC5-6 | 12.4 | 323 | 2.1 | 76.2 | 26.6 | 70.4 |

[a] From solution $^{13}C$ NMR analysis. [b] From DSC thermograms recorded at a scanning rate of 10 °C $min^{-1}$.

## Results and discussion

Fig. 1 shows the DSC curves recorded at 10 °C $min^{-1}$ during the first heating of the as-prepared samples (A), successive cooling from the melt (B) and heating of the melt-crystallized samples (C) of iPP and iPPC5 copolymers. The values of melting temperatures of the as-prepared ($T_m^I$) and melt-crystallized ($T_m^{II}$) samples, and crystallization temperatures ($T_c$) evaluated from the DSC curves in Fig. 1, are reported in Table 1. All samples crystallize from the melt at the employed scan rate and both melting and crystallization temperatures progressively decrease with increasing pentene concentration.

X-ray diffraction profiles of samples crystallized by cooling from the melt as shown in the DSC curves of Fig. 1B are reported in Fig. S1 of the ESI.† Samples with pentene concentrations in the range of 0.55–10.5 mol% basically crystallize from the melt in the α form of iPP, as indicated by the presence of the $(110)_\alpha$, $(040)_\alpha$ and $(130)_\alpha$ reflections at $2\theta$ = 14, 17 and 18.6° of the α form in the diffraction profiles of Fig. S1.† A small amount of the γ form crystallizes in the copolymers with low pentene concentrations, as indicated by the presence of the $(117)_\gamma$ reflection of the γ form at $2\theta$ = 20.1° of low intensity in the diffraction profiles a–d of Fig. S1.† Moreover, a small amount of the δ form crystallizes in the sample with 10.5 mol% of pentene, as indicated by the presence of the small reflection at $2\theta$ = 10.5° in the diffraction profile e of Fig. S1.† [29,31] Finally, the X-ray diffraction profile of the sample with 12.4 mol% (profile f of Fig. S1†) totally changes presenting only the three $(110)_\delta$, $(300)_\delta$ and $(211)_\delta$ + $(220)_\delta$ reflections at $2\theta$ = 10.5°, 18.3° and 21° indicating the crystallization of the pure trigonal δ form.[31] The shift of the reflections of the α form towards lower $2\theta$ values with the increase in pentene concentration in the diffraction profiles of Fig. S1† indicates an increase in the unit cell dimensions of the α form and demonstrates the inclusion of pentene comonomeric units in the crystals of the α form.[29,31] The co-crystallization of pentene comonomers induces an increase in crystalline density and consequent crystallization of the δ form in samples of high pentene concentrations.[29,31]

Self-nucleation experiments (SN) have been performed on copolymers and on the homopolymer to evaluate the effect of incorporated pentene units on the melt-memory behavior of iPP. Only the data for iPP homopolymer and the two samples iPPC5-2 and iPPC5-6 with low (2.0 mol%) and high (12.4 mol%) pentene concentrations are reported in Fig. 2, 3 and 4, respectively. The SN experiments for all other copolymers are reported in Fig. S2–S5 of the ESI.† For all samples,

 

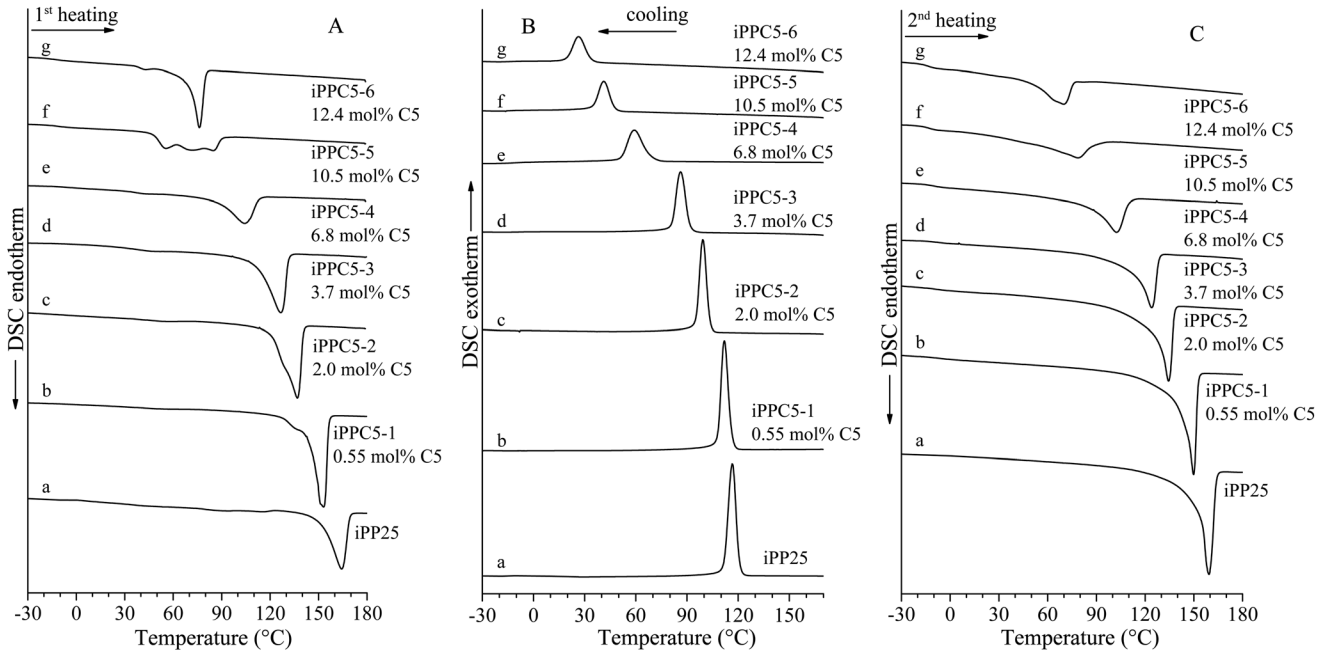


**Fig. 1** DSC thermograms of samples of iPP homopolymer (iPP25) (a) and iPPC5 copolymers of different pentene (C5) concentrations (b–g) recorded at 10 °C $min^{-1}$ during heating of the as-prepared samples (A), cooling from the melt (B), and successive heating of the melt-crystallized samples (C).

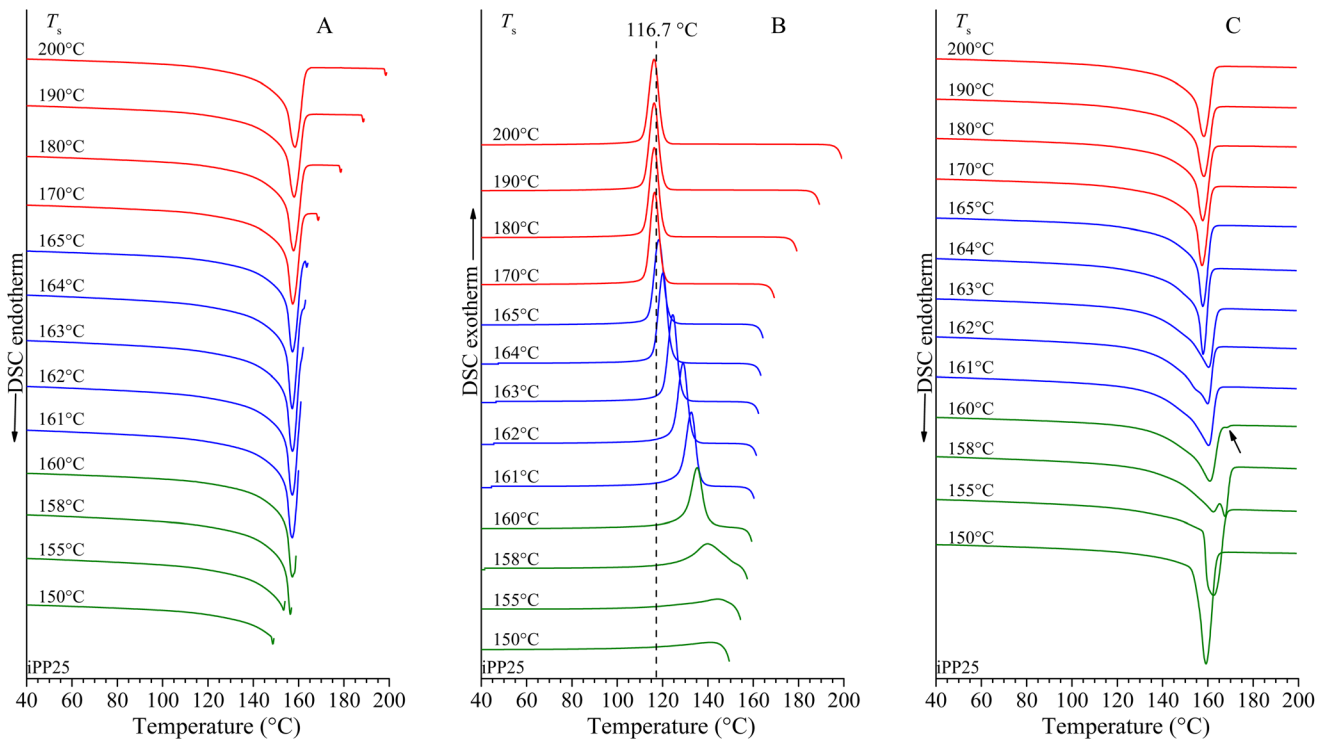


**Fig. 2** DSC curves recorded in the SN experiments for the sample of iPP homopolymer (iPP25), upon heating up to the indicated different seeding temperatures $T_s$ (A), successive cooling after 5 min at $T_s$ down to 25 °C (B) and subsequent heating to melt the self-nucleated crystallized or annealed samples (C). All thermograms are recorded at 10 °C $min^{-1}$. Different colors indicate the different Domains I (red), II (blue) and III (green). The arrow in C indicates the annealing peak.

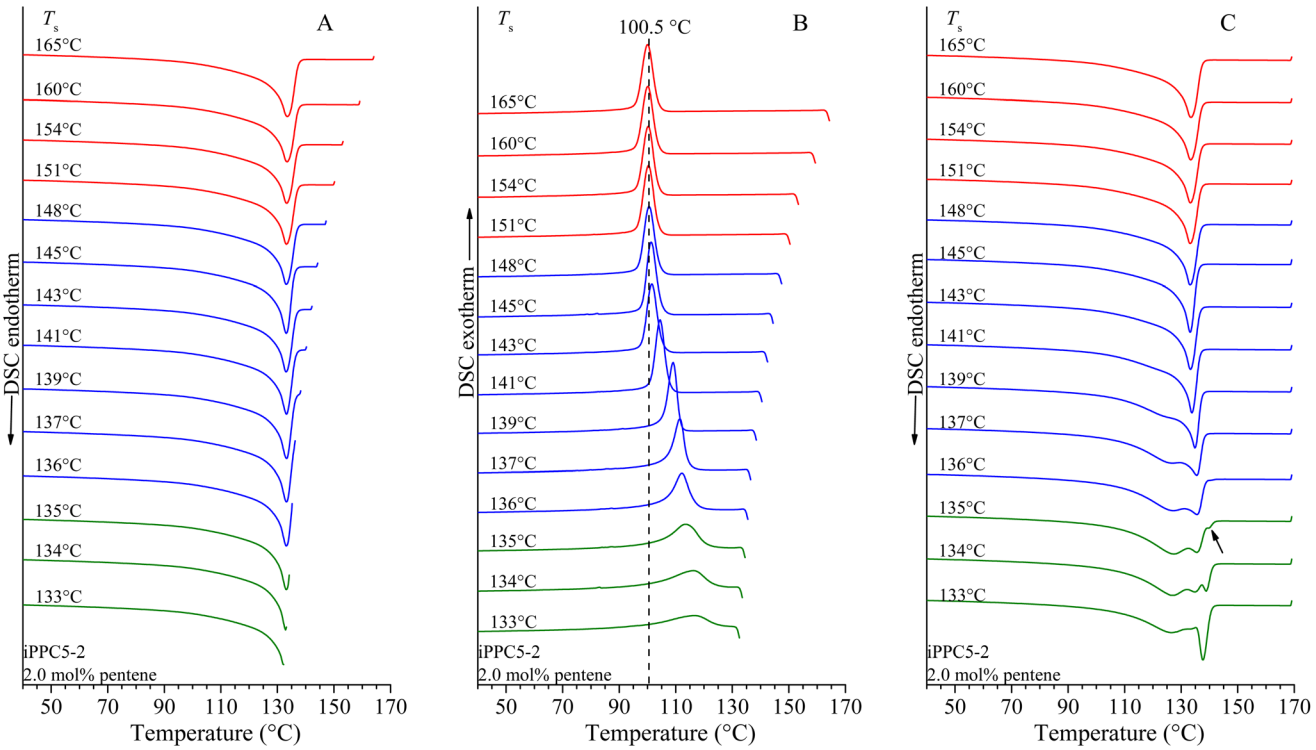


**Fig. 3** DSC curves recorded in the SN experiments for the copolymer sample iPPC5-2 with 2 mol% of pentene, upon heating up to the indicated different seeding temperatures $T_s$ (A), successive cooling after 5 min at $T_s$ down to 25 °C (B) and subsequent heating to melt the self-nucleated crystallized or annealed samples (C). All thermograms are recorded at 10 °C min$^{-1}$. Different colors indicate the different Domains I (red), II (blue) and III (green). The arrow in C indicates the annealing peak.

Fig. 2–4 and Fig. S2–S5† report the DSC heating curves up to the different melt temperatures $T_s$ (Fig. 2A–4A and S2A–S5A†), the cooling thermograms after 5 min at $T_s$ showing crystallization after self-nucleation or annealing at $T_s$ (Fig. 2B–4B and S2B–S5B†) and the successive heating thermograms showing melting of the crystallized self-nucleated (or annealed) samples (Fig. 2C–4C and S2C–S5C†).

As defined by Fillon *et al.*,[9] the crystallization and melting behaviors in SN experiments allow classifying the SN temperatures into three different domains indicated in Fig. 2–4 with distinct colors: red, blue and green for Domains I, II and III, respectively. For the iPP homopolymer sample, at melt temperatures $T_s$ lower than 200 °C and equal to or higher than 170 °C (Fig. 2A), the sample crystallizes by cooling from $T_s$ at the same temperature of 116.7 °C (Fig. 2B) as that in the standard DSC measurement shown in Fig. 1B. In this range of $T_s$, the melt is in the isotropic state of Domain I with no memory of the preceding crystalline phase. Therefore, for the highly stereoregular sample of iPP, the melt-memory is erased already upon heating at temperatures (170 °C) only a few degrees above the end of the endothermic signal $T_{m,end}$ (166 °C, see Fig. 2A).

For $T_s$ lower than 170 °C and higher than or equal to 161 °C, the cooling thermograms from $T_s$ show a remarkable shift of the crystallization peaks toward higher temperatures with decreasing $T_s$ compared to the value of 116.7 °C recorded in Domain I (Fig. 2B). This indicates that in this range of values of $T_s$ the melt is heterogeneous and is in Domain II where the sample experiences self-nucleation. The width of Domain II in terms of $T_s$ ($\Delta T_{s,DII}$) is only 5 °C (from $T_s$ = 165 °C to $T_s$ = 161 °C) and the crystallization temperature increases by 16.5 °C in Domain II, from 116.7 °C in Domain I to the maximum value of 133.2 °C in Domain II (Fig. 2B) at the minimum self-nucleation temperature $T_s$ = 161 °C ($T_{s,ideal}$), where the maximum nucleation density is generated without annealing.[40,41]

At temperatures lower than $T_{s,ideal}$, a low enthalpy endothermic peak appears (annealing peak indicated by an arrow in Fig. 2C) indicating that at these $T_s$ unmolten crystals are annealed and the melt is in Domain III. For iPP, $T_s$ = 160 °C identifies the border between Domains II and III and the enthalpy of the annealing peak increases with decreasing $T_s$ (Fig. 2C), whereas the crystallization temperature of the material molten at $T_s$ that crystallizes upon cooling in Domain III keeps increasing and, finally, decreases with decreasing $T_s$ (Fig. 2B).

Analogous SN behaviors are observed in Fig. 3 and 4 and S2–S5 of the ESI† for the iPPC5 copolymers but with remarkable differences in the temperatures at which the melt-memory persists and values of $T_s$ corresponding to the beginning of Domains II and III. From Fig. 3, it is evident that for the sample iPPC5-2 with 2.0 mol% of pentene, compared to

 

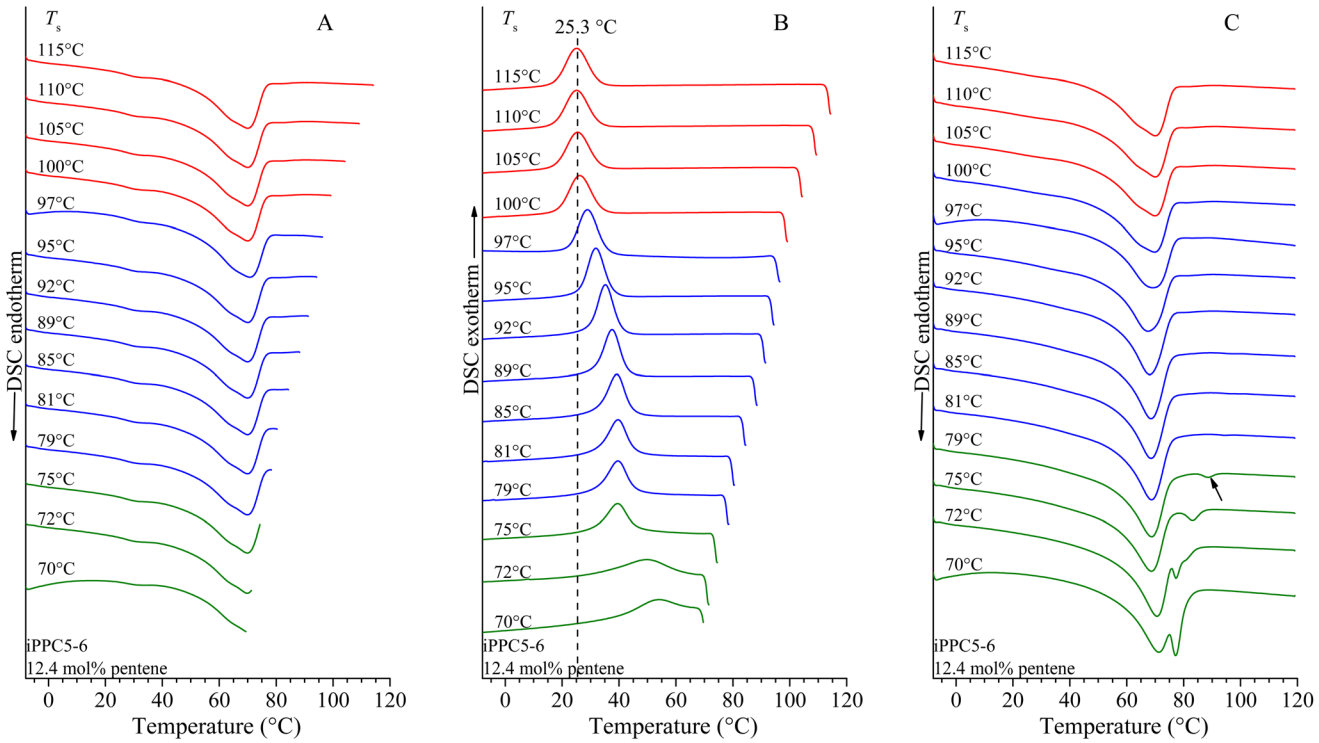


**Fig. 4** DSC curves recorded in the SN experiments for the copolymer sample iPPC5-6 with 12.4 mol% of pentene, upon heating up to the indicated different seeding temperatures $T_s$ (A), successive cooling after 5 min at $T_s$ down to −10 °C (B) and subsequent heating to melt the self-nucleated crystallized or annealed samples (C). All thermograms are recorded at 10 °C min$^{-1}$. Different colors indicate the different Domains I (red), II (blue) and III (green). The arrow in C indicates the annealing peak.

iPP, the memory of the previous crystalline phase is completely erased (the starting of Domain I) only for high $T_s$ temperatures, equal to or higher than 151 °C (Fig. 3A,B), that is, 9–10 degrees above the end of the endothermic signal (140 °C, Fig. 3A). In this temperature range, the crystallization temperature upon cooling from $T_s$ is constant at around 100 °C (Fig. 3B), as in the DSC standard measurements reported in Fig. 1B, and the melt is in Domain I. For $T_s$ lower than 151 °C and higher than 135 °C, the crystallization temperature increases over 13 °C compared to that recorded in Domain I (Fig. 3B) and the sample is in self-nucleation Domain II. Finally, for $T_s$ equal to 135 °C, the appearance of the small annealing peak in the heating DSC curve of Fig. 3C identifies the frontier of Domains II and III. For $T_s$ lower than 135 °C, the sample is in Domain III (annealing domain) and the enthalpy of the annealing peak keeps increasing with decreasing $T_s$ (Fig. 3C).

The differences between the SN behaviors of copolymers and the homopolymer are amplified with the increase of pentene concentration, and in the sample iPPC5-6 with 12.4 mol% of pentene, an outstanding memory effect has been surprisingly observed. Fig. 4 shows that this sample melts under standard conditions at 70 °C (Table 1 and Fig. 1C and 4A) with the end of the endothermic signal at nearly $T_{m,end}$ = 78 °C, but the memory of the crystals persists up to much higher temperatures and is erased only at 100 °C, that is 22 °C above $T_{m,end}$ (Fig. 4A). For $T_s$ values higher than 100 °C, the sample crystallizes by cooling at the sameconstant temperature of 25.3 °C (Fig. 4B) as in the standard DSC measurements reported in Fig. 1B, and the melt is in Domain I. For $T_s$ values lower than 100 °C and higher than 79 °C the crystallization temperature increases with decreasing $T_s$ and the sample is in self-nucleation Domain II (Fig. 4B). Finally, for $T_s$ = 79 °C, the annealing peak appears in the heating scan of Fig. 4C, indicating the boundary between Domains II and III. For $T_s$ lower than 79 °C, the sample is in Domain III (annealing domain), and the enthalpy of the annealing peak keeps increasing with decreasing $T_s$ (Fig. 4C). These data indicate that while the highly stereoregular iPP homopolymer shows a small memory effect in the melt, iPPC5 copolymers show a remarkable memory that persists in the melt up to temperatures much higher than the end of the endothermic signal, and the higher the amount of pentene comonomeric units and the lower the melting temperature, the higher the temperature that must be reached to dissolve the self-nuclei and erase the melt-memory. This result is surprising and rather puzzling because in copolymers of olefins, the melt-memory has been associated with and attributed mainly to non-crystallizable comonomers mainly rejected from the crystalline phase.[11,23,24] In our system, pentene units are instead largely included in the crystals of the α and δ forms of iPP.

The crystallization temperatures evaluated from the cooling thermograms in Fig. 2B–4B and S2B–S5B† are reported in Fig. 5 as a function of the nucleation temperature $T_s$ for all the

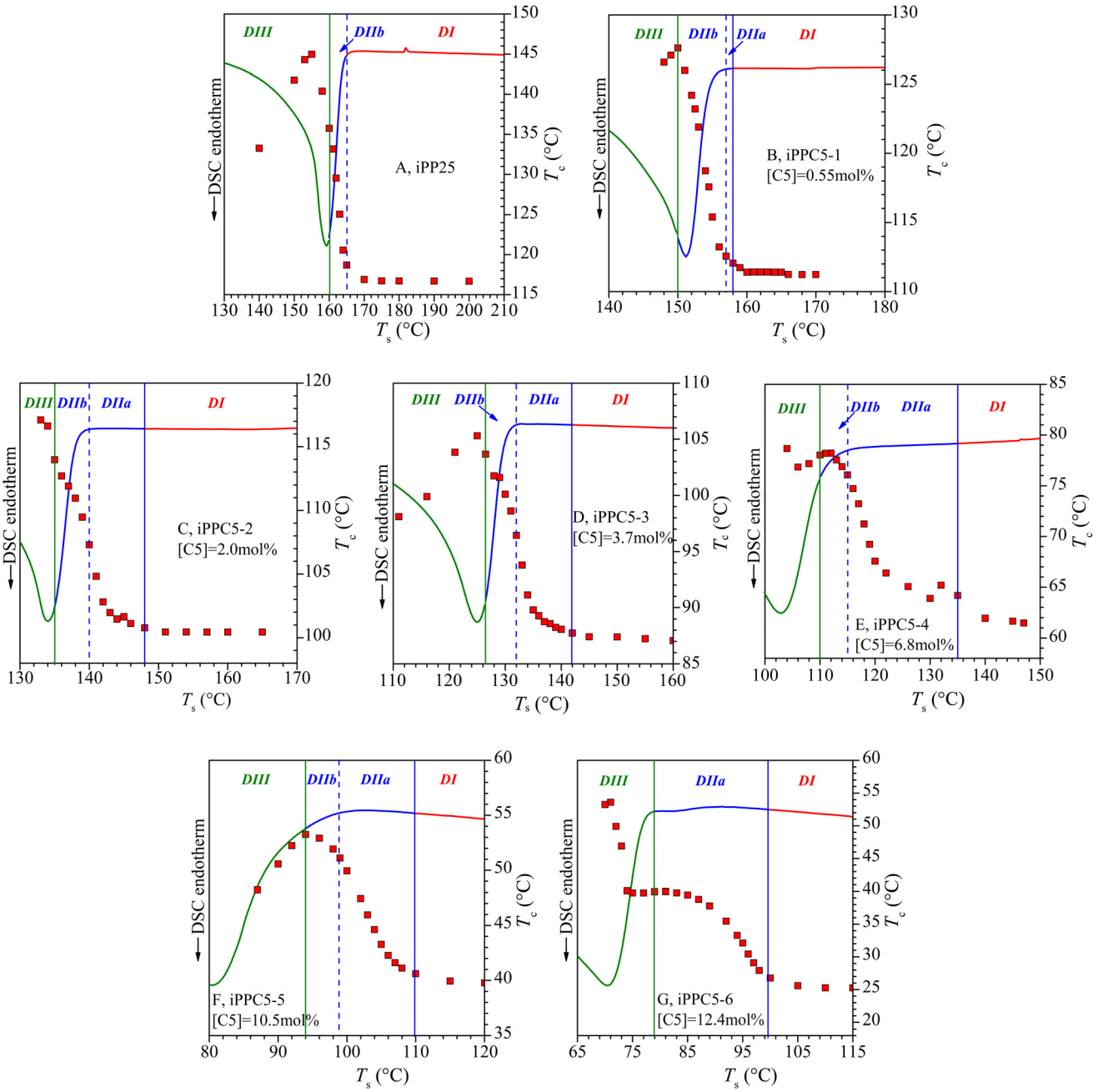


**Fig. 5** Values of crystallization temperatures $T_c$ as a function of the seeding temperatures $T_s$ of the iPP homopolymer (iPP25) and iPPC5 copolymers of different pentene (C5) concentrations, evaluated from the SN cooling scans of Fig. 2B–4B and S2B–S5B.† The plots are superposed to the DSC heating thermograms of Fig. 1C of melt-crystallized samples. The vertical lines indicate the boundary temperatures between the different Domains I (*DI*), II (*DII*) and III (*DIII*). The vertical dashed lines at the end of the endotherms indicate the separation of Domain II into Domain IIa (*DIIa*) and Domain IIb (*DIIb*).

analyzed samples. The plots are overlaid on the "standard" DSC second melting curve of the samples, to show the location of the different domains compared to the melting endotherms. The crystallization temperatures for all samples are compared in Fig. 6 as a function of $T_s$. As already mentioned, these data indicate that different samples with different concentrations of pentene comonomer units show different values of $T_s$ corresponding to the starting of Domains II and III, different widths of Domain II ($\Delta T_{s,DII}$), different ideal self-nucleation temperatures $T_{s,ideal}$ and different increases in crystallization temperature within Domain II. These parameters of SN experiments for all samples are reported in Table 2 and in Fig. 7 as a function of the pentene concentration.

Particularly relevant are the values of the temperature $T_s$ associated with the boundary between Domains I and II

 

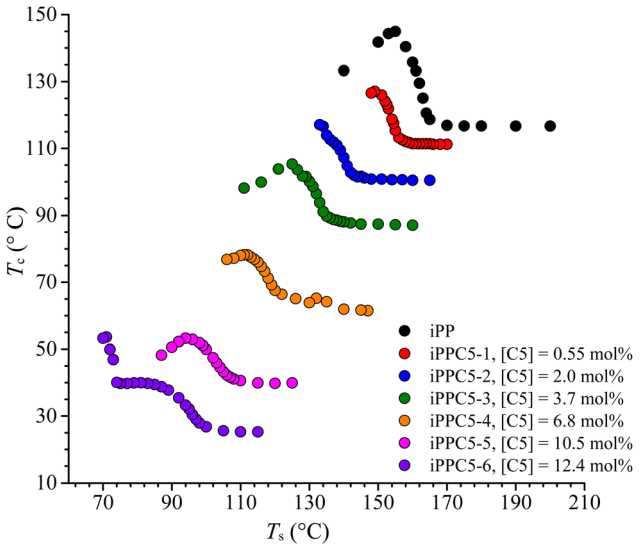


**Fig. 6** Values of crystallization temperatures of iPP homopolymer and iPPC5 copolymers of different concentrations of pentene (C5) units, evaluated from the DSC cooling thermograms from the melt at different nucleation temperatures $T_s$ of Fig. 2B–4B and S2B–S5B,† as a function of $T_s$.

($T_{s,DI-DII}$) that indicates the starting of Domain II, below which the melt is heterogeneous with self-nuclei and above which the memory of the crystalline state is erased, and the width of Domain II in terms of range of $T_s$ temperatures ($\Delta T_{s,DII}$). It is evident from Fig. 5 that the sample iPPC5-1 with the lowest pentene content (0.55 mol%) shows a behavior similar to that of the homopolymer, although a slight widening of Domain II compared to the homopolymer is already observed (Fig. 5A, B and 7A, B). The boundary temperature between Domains I and II ($T_{s,DI-DII}$) decreases with increasing pentene concentration, parallel to the decrease in the melting temperature (Fig. 7A), but, nevertheless, for high pentene concentrations, this boundary temperature $T_{s,DI-DII}$ is much higher than the temperature corresponding to the end of the melting endotherm $T_{m,end}$ and the difference $T_{s,DI-DII} - T_{m,end}$ increases with increasing pentene content (Table 2 and Fig. 7D). This indicates that for copolymers with high pentene concentrations Domain II begins at very high temperatures compared to the melting temperature and, therefore, the melt-memory is preserved at temperatures much higher than the end of the endothermic melting signals as the pentene concentration increases. The temperature corresponding to the end of Domain II with the transition into Domain III ($T_{s,DII-DIII}$), as expected, regularly decreases with increasing pentene concentration and decreasing melting temperature (Fig. 7A). Consequently, the width of Domain II in terms of range of values of $T_s$ becomes larger with increasing pentene concentration (Fig. 7A and B).

As suggested by Muller *et al.*,[11] Domain II may be split into two sub-domains, Domain IIa and Domain IIb. In the Domain IIa, which comprises the high-temperature part of the Domain II, the melt-memory is attributed to the persistence of self-nuclei represented by some chain aggregation or residual ordered chain conformations. The Domain IIb, instead, is placed at low $T_s$ of the endotherm and is distinguished by the presence of small fragments of crystals that behave as self-seeds, which, compared to self-nuclei, are more oriented and ordered. For the iPP homopolymer and the copolymer sample iPPC5-1 with low pentene concentration, Domain II consists basically only of Domain IIb (Fig. 5A and B).

The noticeable increase in the width of Domain II with the increase in pentene content, from 8 °C for the sample with the lowest pentene concentration to ≈21 °C for the sample characterized by the highest pentene content of 12.4 mol% (Table 2), is mainly due to the appearance and gradual widening of Domain IIa (Fig. 5B–G). The width of Domain IIb, instead, does not change or slightly decreases with increasing pentene content and drops to zero in the sample with 12.4 mol% of pentene (Fig. 5B–G and 7B). In this sample, indeed, Domain IIb disappears and Domain II is entirely made of Domain IIa (Fig. 5G and 7B), which extends up to 100 °C, about 30 °C over the melting peak temperature (70 °C) and more than 20 °C over the end of the melting endotherm (Fig. 5G and 7D). For this sample, self-nucleation without annealing exclusively occurs for seeding temperatures higher than the end of the melting endotherm. The increase in crystallization temperature inside Domain II is on average of nearly 15 °C for all samples (Fig. 7C).

As already discussed in the introduction, similar behavior has already been observed in isotactic propylene–ethylene

**Table 2** Concentrations of pentene comonomeric units (mol%), melting temperatures of melt-crystallized samples ($T_m^{II}$) and temperatures corresponding to the end of the melting endotherm ($T_{m,end}$), boundary temperatures between Domains I and II ($T_{s,DI-DII}$) and Domains II and III ($T_{s,DII-DIII}$), widths of Domain II ($\Delta T_{s,DII}$), Domain IIa ($\Delta T_{s,DIIa}$) and Domain IIb ($\Delta T_{s,DIIb}$) and increase in the crystallization temperature inside Domain II ($\Delta T_{c,DII}$), evaluated from SN experiments of iPP homopolymer (iPP25) and iPPC5 copolymers

| Sample | Pentene (mol%) | $T_m^{II}$ (°C) | $T_{m,end}$ (°C) | $T_{s,DI-DII}$ | $T_{s,DII-DIII}$ | $\Delta T_{s,DII}$ | $\Delta T_{s,DIIa}$ | $\Delta T_{s,DIIb}$ | $\Delta T_{c,DII}$ |
|---|---|---|---|---|---|---|---|---|---|
| iPP25 | 0 | 159.8 | 165 | 165 | 160 | 5 | 0 | 5 | 19.0 |
| iPPC5-1 | 0.55 | 149.8 | 157 | 158 | 150 | 8 | 1 | 7 | 14.8 |
| iPPC5-2 | 2.0 | 134.4 | 140 | 148 | 135 | 13 | 8 | 5 | 12.2 |
| iPPC5-3 | 3.7 | 124.2 | 132 | 142 | 126.5 | 15.5 | 10 | 5.5 | 14.6 |
| iPPC5-4 | 6.8 | 102.4 | 115 | 135 | 110 | 25 | 20 | 5 | 16.7 |
| iPPC5-5 | 10.5 | 79.3 | 99 | 110 | 94 | 16 | 11 | 5 | 13.0 |
| iPPC5-6 | 12.4 | 70.4 | 79 | 100 | 79 | 21 | 21 | 0 | 14.7 |

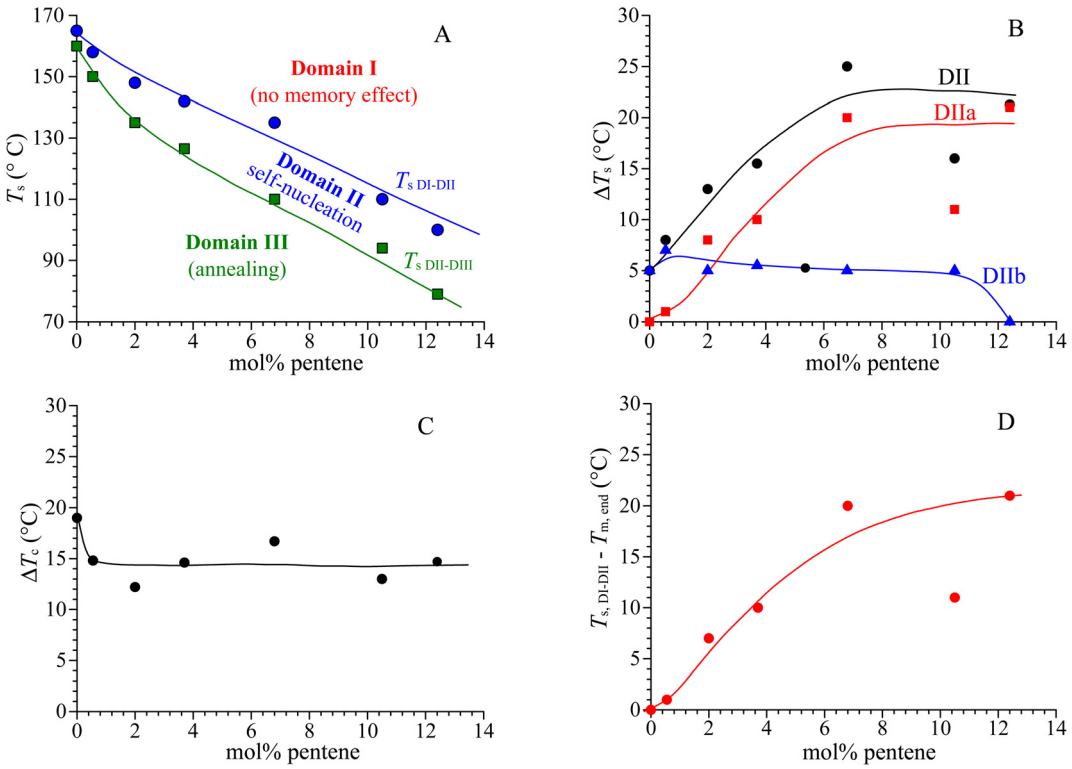


**Fig. 7** Boundary temperatures between Domains I and II ($T_{s,DI-DII}$) (●) and Domains II and III ($T_{s,DII-DIII}$) (■) (A), widths of Domain II (●), Domain IIa (■) and Domain IIb (▲) ($\Delta T_s$) (B), increase of the crystallization temperature inside Domain II ($\Delta T_c$) (C) and the difference between the boundary temperature of Domains I and II and the temperature corresponding to the end of the melting endotherm ($T_{s,DI-DII} - T_{m,end}$) (D), evaluated from the SN experiments in iPPC5 copolymers, as a function of the pentene concentration.

copolymers[15] and, more recently, in iPP-based functional copolymers with a bulky amino-functionalized comonomer.[25] In both cases, the persistence of memory in the melt up to very high temperatures and the broadening of Domain II have been explained by the mechanism proposed for statistical copolymers of PE with non-crystallizable comonomers[23,24] and attributed to the formation, in the melt, of clusters of chains or segments which remain upon melting.[23,24] This aggregation of clusters of chains and the resulting melt heterogeneity would originate during the crystallization of statistical copolymers by the partitioning of crystallizable sequences of suitable lengths during crystallization and the selection of more regular and longer sequences during crystal growth.[23,24,27,42] The rejection of comonomers from the crystals and the consequent early selection of longer crystallizable sequences during crystallization would require the later diffusion of shorter sequences from the melt toward the crystal growth front, forming restrictions in the melt (knots, loops and ties). These constraints prevent, during successive melting, the diffusion and homogenization of all sequences leaving clusters of sequences or segments in the melt that are erased only at very high temperatures. These clusters represent the self-nuclei that give nucleation during crystallization from the melt.[11,15,23–25] According to this proposed mechanism, memory effects have not been observed in PE and iPP homopolymers,[23,24,27,42] as also demonstrated by our data in Fig. 2 and 5A.

However, this mechanism accounts for the behaviors shown by statistical copolymers with non-crystallizable comonomeric units largely rejected from the crystals.[11] Our data in Fig. 2–7 demonstrate that a remarkable melt memory of iPP crystals, which persists in the melt up to high temperatures, is present not only for copolymers with noncrystallizable comonomers but also for comonomers largely included in the crystals, such as pentene comonomer units, which at high comonomer concentrations even co-crystallize with propene. This result is rather surprising also considering that exactly the opposite result has been observed in the literature for other systems, such as copolyesters, where the incorporation of comonomers within crystals reduces or even erases the melt-memory.[43,44] However, as mentioned in the introduction, in polar polymers such as polyesters, poly(amides), polycarbonates or polyethers that contain several functional groups, the melt memory is directly related to the presence and strength of intermolecular interactions, such as dipole interactions or hydrogen bonds.[11,21,22,44–48] The stronger the interactions, the more pronounced the melt memory effect and the higher the increase in crystallization temperature in comparison with the standard crystallization temperature.[11,21,22,44–48] The disappearance of the melt-memory in isodimorphic copolyesters, where two comonomers co-crystallize in the same unit cell, has been interpreted as due to the disruption of inter-

 

molecular interactions.[43,44] In our apolar iPPC5 copolymers, the melt-memory is not due to intermolecular interactions and the co-crystallization of pentene units does not involve changes in molecular interactions.

As mentioned above, pentene comonomeric units are largely included in the crystallizable propene sequence but they are anyway distributed between amorphous and crystalline phases. The partitioning coefficients $P_{CR}$, that is the ratio between the amount of comonomer units in the crystalline state and the total concentration, have been determined by Hosoda *et al.*[49] for propene–butene, propene–hexene and propene–octene copolymers by $^{13}$C NMR spectroscopy on copolymer samples etched with fuming nitric acid. In this method, amorphous chains are assumed to be completely removed by etching and it was possible to determine the amount of comonomers included in crystals through the $^{13}$C NMR spectrum of the residue after etching. They reported that hexene and butene are almost equally distributed between amorphous and crystalline phases with values of $P_{CR}$ close to 0.5, which increase with the total concentration of comonomer units.[49] It is reasonable to assume a similar partitioning ratio of nearly 0.5 in propene-pentene copolymers, with pentene units almost equally distributed between amorphous and crystalline phases. Therefore, during the crystallization of iPPC5 copolymers, the selection of crystallizable sequences should be less demanding, but during the melting at low temperatures of these defectively formed crystals containing a high amount of pentene units, the diffusion and homogenization of all sequences are anyhow challenging, also because of the low temperature, and segments of partitioned sequences are left in the melt, acting as self-nuclei during cooling and crystallization from the melt, in accordance with the proposed mechanism.[23,24]

Self-nucleation can influence the polymorphic behavior of a polymeric material and sometimes can induce the crystallization of a particular polymorphic form rather than another.[28,50,51] For iPPC5 copolymers[37] and copolymers of iPP in general,[38,52–60] the crystallization of the α and γ forms strongly depends on crystallization conditions and the possible inclusion of comonomer units in the crystals or their rejection, which, in turn, depends on the type and size of the defect. The effect of the presence of melt-memory and the occurrence of self-nucleation on the polymorphic behaviors of iPPC5 copolymers have been analyzed by recording X-ray diffraction profiles on selected samples crystallized by cooling from different values of $T_s$ belonging to the three different domains. The resulting diffraction profiles for selected values of $T_s$ are reported in Fig. 8. The crystallized samples are obtained after the DSC cooling steps of the SN experiments in Fig. 2B–4B and S2B–S5B.† As in the cooling curves, the different colors in Fig. 8 correspond to different domains. All samples crystallize in mixtures of α and γ forms, as indicated by the presence of the $(130)_\alpha$ and $(117)_\gamma$ reflections at $2\theta$ = 18.6° and 20.1° of the α and γ forms, respectively, and the α form prevails in the crystallization from high $T_s$ temperatures belonging to Domain I (Fig. 8). Samples with low pentene concentration ranging from 0.5 to 3.7 mol% develop a low amount of the γ form (10–20%), which remains almost constant throughout Domain I (Fig. 8A–C). Even the samples with high contents of pentene crystallize from the homogeneous Domain I mainly in the α form (Fig. 8D and E).

In all samples, the amount of the γ form increases with the decrease in $T_s$ when crystallization occurs from temperatures belonging to Domain II with self-nucleation (Fig. 8), achieves a maximum for $T_s$ values of Domain IIb and then slightly decreases for further decrease in $T_s$ when crystallization occurs from Domain III (Fig. 8). Samples iPPC5-4 and iPPC5-5 with a pentene concentration of 6.8 and 10.5 mol%, respectively, show similar behavior but crystallize only in the α form for $T_s$ included in Domain I and develop the maximum amount of the γ form for seeding temperatures no longer belonging to Domain II but included in Domain III (Fig. 8D and E). In particular, the sample iPPC5-5 with 10.5 mol% of pentene develops an amount of γ form lower than that obtained for the samples with lower pentene content. The sample iPPC5-6 with 12.4 mol% of pentene crystallizes in α and δ forms at any investigated $T_s$ temperatures and no traces of the γ form are present (Fig. 8F). In particular, this sample crystallizes essentially in the δ form for high $T_s$ temperatures of Domain I and a small amount of the α form crystallizes for lower $T_s$ temperatures belonging to Domains II and III, which then increases with decreasing $T_s$. At the lowest $T_s$ (70 °C), an almost pure trigonal δ form crystallizes (Fig. 8F). In any case, the γ form never crystallizes for the highest pentene concentration.

The fractional amount of the γ form, with respect to the α form, that crystallizes in all samples at different $T_s$ temperatures is reported in Fig. 9A as a function of $T_s$. It is apparent that for each sample, the amount of the γ form increases with decreasing $T_s$ and the maximum amount ($f_\gamma$(max)) is achieved at different values of $T_s$ that depend on the pentene concentration. For different samples, the maximum amount of the γ form is obtained at decreasing values of $T_s$ with increasing pentene concentration due to the shift of Domain II toward lower temperatures. The maximum amount of the γ form $f_\gamma$(max) that crystallizes for each sample in the SN experiments (the maxima of the curves in Fig. 9A) is reported in Fig. 9B as a function of the pentene concentration. It is evident that at small pentene concentrations, $f_\gamma$(max) rapidly increases up to a constant maximum value of about 70% for a pentene concentration of 2 mol%, then remains constant up to 6–7 mol% of pentene and, finally, quickly decreases with the increase in pentene concentration and is null for pentene concentrations higher than 12 mol% (Fig. 9B). As already mentioned, the sample iPPC5-6 with 12.4 mol% of pentene, indeed, crystallizes only in α and δ forms at any $T_s$ temperatures without traces of the γ form (Fig. 8F).

These data indicate that under analogous conditions of cooling rate, for iPPC5 copolymers with small pentene concentrations up to 6–7 mol%, the presence of memory in the melt and the occurrence of self-nucleation favor the crystallization of the γ form, whereas crystallization from a homogeneous melt under standard conditions favors the crystallization of

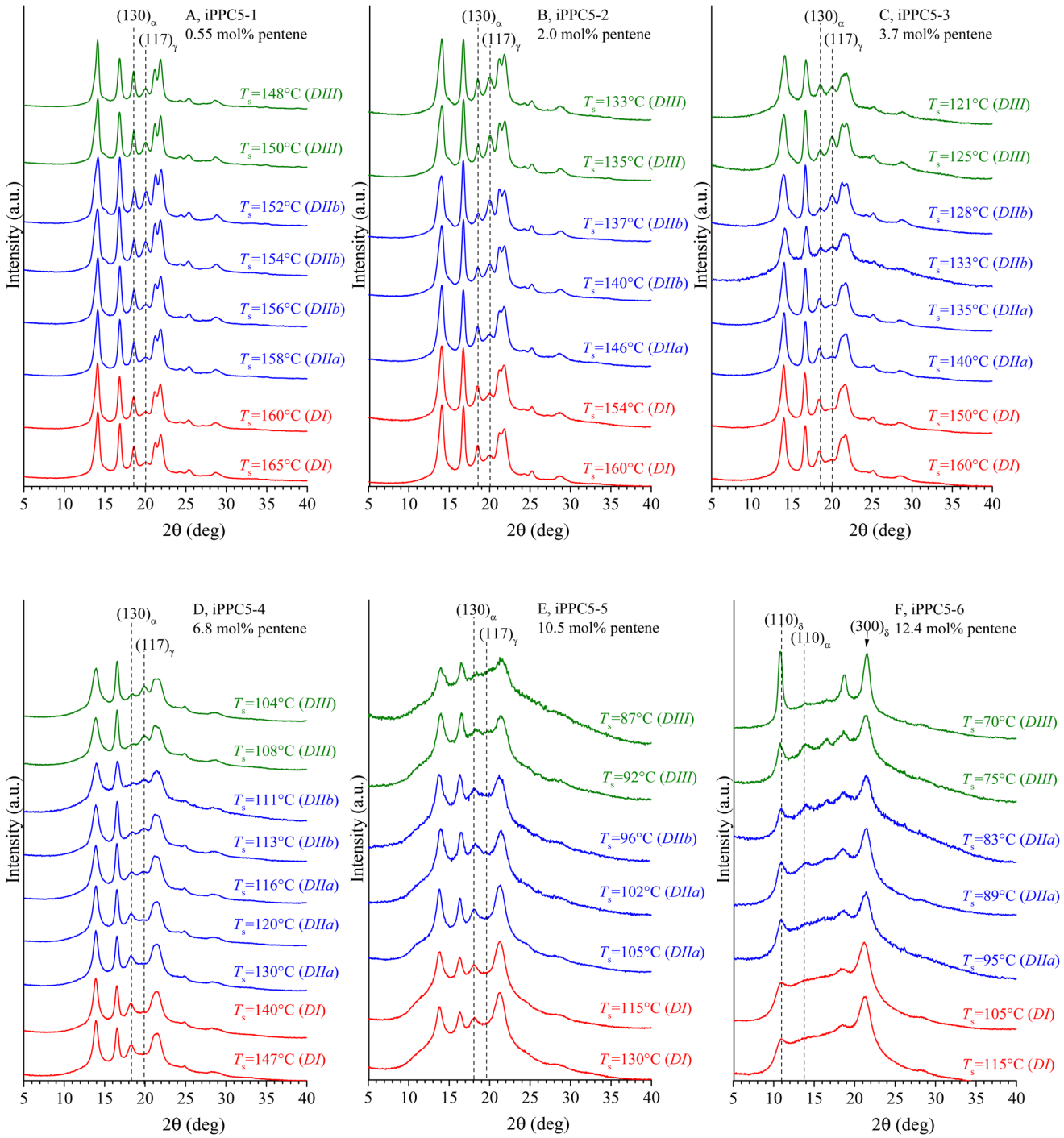


**Fig. 8** X-ray powder diffraction profiles of samples of iPPC5 copolymers crystallized by cooling from the melt at 10 °C $min^{-1}$ from different seeding temperatures $T_s$ of the melt belonging to the three Domains DI, DII and DIII. The $(130)_\alpha$ and the $(117)_\gamma$ reflections of the α and γ forms of iPP at $2\theta$ = 18.6° and 20.1° are indicated. In (F), the $(110)_\delta$ and $(300)_\delta$ reflections at $2\theta$ = 10–11° and 18–19° of the δ form are also indicated.

the α form, even for pentene concentrations of 5–6 mol% that should favor the crystallization of the γ form. Therefore, self-nuclei characterized by clusters with partial chain orientation and conformational order or self-seeds due to the survival of small crystalline fragments that characterize Domains IIa and IIb, respectively, act as nucleating agents for the γ form of iPP, which, indeed, crystallizes in a relative amount much higher than that observed under dynamic cooling conditions from a homogeneous melt (Fig. S1†). Moreover, since in all cases, the amount of the γ form that is obtained for $T_s$ included in Domain III always exceeds that observed in Domain I, it is probable that the α form crystals that remain unmelted and

 

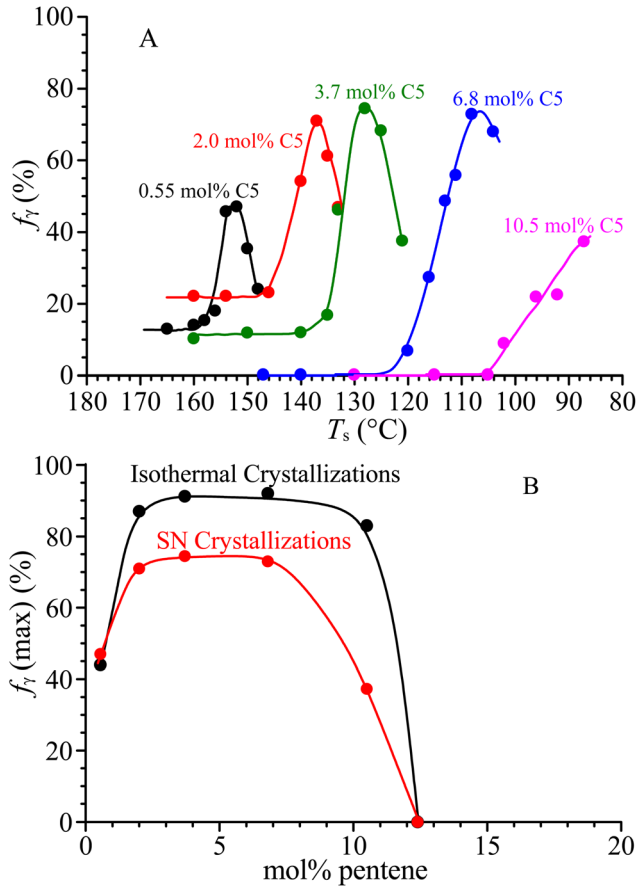


**Fig. 9** (A) Values of the relative amount of the γ form ($f_\gamma$) that crystallizes from the melt in iPPC5 copolymers of different pentene (C5) concentrations in the cooling step of the SN experiments at 10 °C min$^{-1}$ from different seeding temperatures $T_s$, as a function of the seeding temperature $T_s$. (B) Values of the maximum relative amount of the γ form ($f_\gamma$(max)) (the maxima of the curves in A) obtained in iPPC5 copolymers in the SN experiments (●) as a function of pentene concentration compared with that achieved for the same samples isothermally crystallized from the melt at different crystallization temperatures (●).[37]

only experience annealing for low seeding temperatures also act as nucleating agents for the crystallization of the γ form. For pentene concentrations higher than 6–7 mol%, the high amount of pentene comonomer units included in the crystals of α and δ forms favors the crystallization of the α form and of the pure trigonal δ form for the highest pentene concentration, even for $T_s$ temperatures of Domain II with self-nucleation.

The plot of Fig. 9 reminds us of analogous literature plots of the amount of the γ form that crystallizes in the same iPPC5 copolymers in isothermal crystallizations from the melt at different crystallization temperatures,[37] and in other copolymers of iPP with different comonomers.[38,52,53,55–60] These literature data demonstrate that iPPC5 copolymers crystallize in isothermal crystallization from the melt in mixtures of α and γ forms and the amount of the γ form increases with increasing crystallization temperature and for different samples, a maximum amount of the γ form is obtained at different crystallization temperatures.[37] The maximum amount of the γ form that crystallizes in isothermal crystallizations is different for different samples of copolymers and increases with increasing pentene concentration up to 6–7 mol% of pentene; then, it decreases for higher pentene content because of the favored crystallization of the δ form.[37] The maximum relative amount of the γ form $f_\gamma$(max) that crystallizes in isothermal crystallizations, taken from ref. 37, are compared in Fig. 9B with those obtained in this paper on the same samples in nonisothermal crystallizations by cooling from different $T_s$ temperatures of the melt. The two behaviors are perfectly parallel and also in isothermal crystallizations, the maximum amount of the γ form $f_\gamma$(max) rapidly increases up to a highest amount of 90% for a low pentene concentration of 2 mol%, remains constant up to 6–7 mol% of pentene and, then, quickly decreases with the increase in pentene content and is null for pentene concentrations higher than 12 mol%. The only difference is the slightly higher maximum amount of the γ form that crystallizes in isothermal crystallizations (90%) compared to that crystallized in nonisothermal crystallizations by self-nucleation (70%). Therefore, the data in Fig. 9B indicate that under conditions of relatively fast crystallization from the melt by cooling at 10 °C min$^{-1}$ that generally favor the crystallization of the α form even for high contents of constitutional irregularities, a high amount of the γ form, analogous to that crystallized in slow isothermal crystallizations, crystallizes by self-nucleation when melt-memory is retained in the melt.

## Conclusions

The self-nucleation and memory of the crystals in the melt of iPPC5 copolymers have been analyzed. Samples with pentene concentrations varying from 0.5 to 12.4 mol% have been prepared with a highly stereoselective metallocene catalyst. Pentene comonomeric units are largely included in the crystals of the polymorphic forms of iPP and the relative amount of included comonomer increases with the increase in pentene concentration, inducing crystallization of the δ form of iPP when the pentene concentration exceeds about 9–10 mol%.

Self-nucleation experiments have demonstrated that high contents of pentene comonomeric units produce a remarkable melt-memory that survives at temperatures much higher than the melting temperature. The width of Domain II, where self-nucleation occurs, and the difference between the temperature of the beginning of the homogeneous melt, where the melt-memory is erased, and the temperature corresponding to the end of the melting endotherm increase with increasing pentene concentration. The higher the amount of pentene comonomeric units and the lower the melting temperature, the higher the temperature that must be reached to dissolve the self-nuclei and erase the melt-memory.

These data indicate that a remarkable melt-memory of iPP crystals exists not only for the known cases of iPP copolymers with noncrystallizable comonomers but also for copolymers with comonomers largely included in the crystals and that,

hence, cocrystallize inside the propene sequences. According to the mechanism of partitioning of crystallizable sequences and the formation of a constrained melt with clusters of chains acting as self-nuclei,[23,24] and considering that pentene units are equally partitioned between amorphous and crystalline phases, the selection of crystallizable sequences of suitable lengths should be less demanding, but during melting at low temperatures of the highly defective formed crystals incorporating a high amount of constitutional defects, the diffusion and homogenization of all sequences are anyhow more difficult, also because of the low temperature, and segments of partitioned sequences are left in the melt, acting as efficient self-nuclei during cooling and crystallization.

Crystallization from the heterogeneous melt containing self-nuclei favors the crystallization of the γ form, whereas crystallization from the homogeneous melt favors the crystallization of the α form. For a high pentene concentration of 12.4 mol%, the trigonal δ form crystallizes from the homogeneous melt, whereas a small amount of the α form crystallizes from the heterogeneous melt with self-nucleation and no trace of the γ form is observed.

## Author contributions

F. D. S.: synthesis of the samples and writing original draft. C. D. R.: conceptualization, writing and editing. A. B., A. C., M. S. and F. D. S.: investigation. A. C. and F. D. S.: methodology. All authors have approved the final version of the manuscript.

## Conflicts of interest

There are no conflicts to declare.

## Acknowledgements

The task force "Polymers and Biopolymers" of the University of Napoli Federico II is acknowledged.

## References

1 K. A. Mauritz, E. Baer and A. J. Hopfinger, *J. Polym. Sci., Part D: Macromol. Rev.*, 1978, **13**, 1.
2 J. C. Wittmann and B. Lotz, *J. Polym. Sci., Polym. Phys. Ed.*, 1981, **19**, 1837.
3 R. Xin, J. Zhang, X. Sun, H. Li, Z. Qiu and S. Yan, *Adv. Polym. Sci.*, 2015, **277**, 55.
4 C. De Rosa, R. Di Girolamo, A. Malafronte, M. Scoti, G. Talarico, F. Auriemma and O. Ruiz de Ballesteros, *Polymer*, 2020, **196**, 122423.
5 R. L. Miller, *Flow-Induced Crystallization in Polymer Systems*, Gordon and Breach Science, New York, NY, USA, 1977.
6 L. Li and W. H. De Jeu, *Adv. Polym. Sci.*, 2005, **181**, 75.
7 G. Vidotto, D. Levy and A. J. Kovacs, *Kolloid Z. Z. Polym.*, 1969, **230**, 289.
8 J. Xu, Y. Ma, W. Hu, M. Rehahn and G. Reiter, *Nat. Mater.*, 2009, **8**, 348.
9 B. Fillon, J. C. Wittmann, B. Lotz and A. Thierry, *J. Polym. Sci., Part B: Polym. Phys.*, 1993, **31**, 1383.
10 R. M. Michell, A. Mugica, M. Zubitur and A. J. Müller, *Adv. Polym. Sci.*, 2016, **276**, 215.
11 L. Sangroniz, D. Cavallo and A. J. Muller, *Macromolecules*, 2020, **53**, 4581–4604.
12 A. T. Lorenzo, M. L. Arnal, J. J. Sánchez and A. J. Müller, *J. Polym. Sci., Part B: Polym. Phys.*, 2006, **44**, 1738–1750.
13 B. Fernández-D'Arlas, J. Balko, R. P. Baumann, E. Pöselt, R. Dabbous, B. Eling, T. Thurn-Albrecht and A. J. Müller, *Macromolecules*, 2016, **49**, 7952–7964.
14 H. Zhang, C. Shao, W. Kong, Y. Wang, W. Cao, C. Liu and C. Shen, *Eur. Polym. J.*, 2017, **91**, 376–385.
15 L. Sangroniz, D. Cavallo, A. Santamaria, A. J. Müller and R. G. Alamo, *Macromolecules*, 2017, **50**, 642.
16 D. Cavallo, L. Gardella, G. Portale, A. J. Müller and G. C. Alfonso, *Polymer*, 2014, **55**, 137–142.
17 D. Cavallo, L. Zhang, I. Sics, G. C. Alfonso, P. Dumas, C. Marco and G. Ellis, *CrystEngComm*, 2016, **18**, 816–828.
18 W. Li, X. Wu, X. Chen and Z. Fan, *Eur. Polym. J.*, 2017, **89**, 241–248.
19 L. Sangroniz, R. G. Alamo, D. Cavallo, A. Santamaria, A. J. Müller and A. Alegría, *Macromolecules*, 2018, **51**, 3663–3671.
20 L. Sangroniz, F. Barbieri, D. Cavallo, A. Santamaria, R. G. Alamo and A. J. Müller, *Eur. Polym. J.*, 2018, **99**, 495–503.
21 I. Arandia, A. Mugica, M. Zubitur, A. Arbe, G. Liu, D. Wang, R. Mincheva, P. Dubois and A. J. Müller, *Macromolecules*, 2015, **48**, 43–57.
22 X. Liu, Y. Wang, Z. Wang, D. Cavallo, A. J. Müller, P. Zhu, Y. Zhao, X. Dong and D. Wang, *Polymer*, 2020, **188**, 122117.
23 B. O. Reid, M. Vadlamudi, A. Mamun, H. Janani, H. Gao, W. Hu and R. G. Alamo, *Macromolecules*, 2013, **46**, 6485–6497.
24 A. Mamun, X. Chen and R. G. Alamo, *Macromolecules*, 2014, **47**, 7958.
25 Y. Liao, L. Pan, Z. Ma, D. Cavallo, G. Liu, D. Wang and A. J. Muller, *Polymer*, 2023, **282**, 126184.
26 X. Zhao, S. Han, W. Song, L. Liu and Y. Men, *Thermochim. Acta*, 2022, **718**, 179392.
27 S. F. Marxsen and R. G. Alamo, *Polymer*, 2019, **168**, 168.
28 Y. Liao, L. Liu, Z. Ma and Y. Li, *Macromolecules*, 2020, **53**, 2088.
29 C. De Rosa, F. Auriemma, G. Talarico and O. Ruiz de Ballesteros, *Macromolecules*, 2007, **40**, 8531.
30 E. Pérez, M. L. Cerrada, R. Benavente and J. M. Gómez-Elvira, *Macromol. Res.*, 2011, **19**, 1179–1185.
31 C. De Rosa, O. Ruiz de Ballesteros, F. Auriemma and M. R. Di Caprio, *Macromolecules*, 2012, **45**, 2749.
32 E. Pérez, J. M. Gómez-Elvira, R. Benavente and M. L. Cerrada, *Macromolecules*, 2012, **45**, 6481.

 

33 F. Auriemma, C. De Rosa, R. Di Girolamo, A. Malafronte, M. Scoti and R. Cipullo, *Polymer*, 2017, **129**, 235.
34 F. Auriemma, C. De Rosa, R. Di Girolamo, A. Malafronte, M. Scoti and C. Cioce, *Adv. Polym. Sci.*, 2017, **276**, 45.
35 C. De Rosa, M. Scoti, F. Auriemma, O. Ruiz de Ballesteros, G. Talarico, A. Malafronte and R. Di Girolamo, *Macromolecules*, 2018, **51**, 3030.
36 C. De Rosa, M. Scoti, F. Auriemma, O. Ruiz de Ballesteros, G. Talarico, R. Di Girolamo and R. Cipullo, *Eur. Polym. J.*, 2018, **103**, 251.
37 M. Scoti, F. De Stefano, R. Di Girolamo, G. Talarico, A. Malafronte and C. De Rosa, *Macromolecules*, 2022, **55**, 241.
38 M. Scoti, F. De Stefano, R. Di Girolamo, A. Malafronte, G. Talarico and C. De Rosa, *Macromol. Chem. Phys.*, 2023, **224**, 2200262.
39 W. Spaleck, F. Kuber, A. Winter, J. Rohrmann, B. Bachmann, M. Antberg, V. Dolle and E. Paulus, *Organometallics*, 1994, **13**, 954.
40 A. J. Müller, R. M. Michell, R. A. Pérez and A. T. Lorenzo, *Eur. Polym. J.*, 2015, **65**, 132–154.
41 A. J. Müller, Z. H. Hernández, M. L. Arnal and J. J. Sánchez, *Polym. Bull.*, 1997, **39**, 465–472.
42 H. Gao, M. Vadlamudi, R. G. Alamo and W. Hu, *Macromolecules*, 2013, **46**, 6498–6506.
43 L. Sangroniz, M. Safari, A. Martinez de Ilarduya, H. Sardon, D. Cavallo and A. J. Müller, *Macromolecules*, 2023, **56**, 7879–7888.
44 R. A. Pérez-Camargo, M. Safari, J. Torres Rodríguez, Y. Liao and A. J. Müller, *Polymer*, 2023, **287**, 126412.
45 R. A. Pérez-Camargo, I. Arandia, M. Safari, D. Cavallo, N. Lotti, M. Soccio and A. J. Müller, *Eur. Polym. J.*, 2018, **101**, 233–247.
46 L. Sangroniz, A. Sangroniz, L. Meabe, A. Basterretxea, H. Sardon, D. Cavallo and A. J. Müller, *Macromolecules*, 2020, **53**, 4874–4881.
47 P. A. Klonos, L. Papadopoulos, M. Kasimatis, H. Iatrou, A. Kyritsis and D. N. Bikiaris, *Macromolecules*, 2021, **54**, 1106–1119.
48 L. Sangroniz, Y.-J. Jang, M. A. Hillmyer and A. J. Müller, *J. Chem. Phys.*, 2022, **156**, 144902.
49 S. Hosoda, H. Hori, K. Yada, M. Tsuji and S. Nakahara, *Polymer*, 2002, **43**, 7451.
50 P. S. Dai, P. Cebe and M. Capel, *J. Polym. Sci., Part B: Polym. Phys.*, 2002, **40**, 1644.
51 D. Cavallo, L. Gardella, G. Portale, J. A. Muller and C. G. Alfonso, *Macromolecules*, 2014, **47**, 870.
52 C. De Rosa, F. Auriemma, O. Ruiz de Ballesteros, L. Resconi and I. Camurati, *Macromolecules*, 2007, **40**, 6600–6616.
53 C. De Rosa, F. Auriemma, O. Ruiz de Ballesteros, D. De Luca and L. Resconi, *Macromolecules*, 2008, **41**, 2172–2177.
54 M. Scoti, F. De Stefano, F. Piscitelli, G. Talarico, A. Giordano and C. De Rosa, *Polymers*, 2022, **14**, 3873.
55 M. Scoti, F. De Stefano, A. Giordano, G. Talarico and C. De Rosa, *Polymers*, 2022, **14**, 4032.
56 M. Scoti, F. De Stefano, R. Di Girolamo, A. Malafronte, G. Talarico and C. De Rosa, *Macromolecules*, 2023, **56**, 1446–1460.
57 I. L. Hosier, R. G. Alamo, P. Esteso, G. R. Isasi and L. Mandelkern, *Macromolecules*, 2003, **36**, 5623–5636.
58 I. L. Hosier, R. G. Alamo and J. S. Lin, *Polymer*, 2004, **45**, 3441–3455.
59 R. G. Alamo, A. Ghosal, J. Chatterjee and K. L. Thompson, *Polymer*, 2005, **46**, 8774–8789.
60 K. Jeon, H. Palza, R. Quijada and R. G. Alamo, *Polymer*, 2009, **50**, 832.